IEEE Access
Multidisciplinary ⋮ Rapid Review ⋮ Open Access Journal

Received 12 January 2023, accepted 19 February 2023, date of publication 1 March 2023, date of current version 8 March 2023.

Digital Object Identifier 10.1109/ACCESS.2023.3250965

RESEARCH ARTICLE

New Parameter Identification Method for Supercapacitor Model

SERGIO MARÍN-COCA[1], AMIR OSTADRAHIMI[2], STEFANO BIFARETTI[2], (Member, IEEE), ELENA ROIBÁS-MILLÁN[1], AND SANTIAGO PINDADO[1]

[1]Instituto Universitario de Microgravedad "Ignacio Da Riva" (IDR/UPM), ETSI Aeronáutica y del Espacio, Universidad Politécnica de Madrid, 28040 Madrid, Spain

[2]Department of Industrial Engineering, University of Rome "Tor Vergata," 00133 Rome, Italy

Corresponding author: Stefano Bifaretti (stefano.bifaretti@uniroma2.it)

This work was supported by the Programa Propio of the Universidad Politécnica de Madrid.

ABSTRACT The paper introduces a straightforward procedure for estimating the electrical parameters of a simple, but reasonably accurate, two-branches model of a supercapacitor (SC). The equivalent electrical circuit model includes the voltage and frequency dependence on the SC's capacitance, neglecting the self-discharge phenomenon, so it is mainly devoted to short and mid-term simulations suitable for most industrial applications. The estimation procedure of the electrical parameters starts by analysing the experimental data achieved by a common constant-current discharge test. Such data are used to build a fitting function which is compared with the analytical solution and numerical approximations for the SC's voltage evolution. Thus, initial estimated values of the electrical parameters are obtained through simple relations and are optimised by implementing the least squares method. The procedure is validated after an easy and fast extraction of the optimal parameters of the two-branches model of an SC. Several tests involving a commercial SC have been carried out in Simulink and the results have been compared against experimental data. A good accuracy of the two-branches model in a wide range of constant-current charging/discharging cycles is reported.

INDEX TERMS Discharge test, model validation, parameter estimation, supercapacitor.

I. INTRODUCTION

Over the past decades, the increasing demand for high-efficiency energy storage technologies has contributed to the development and implementation of supercapacitors (SCs) in many applications [1]. SCs are suitable for supplying energy during high peak power demands, abrupt power variations or temporary power outages, and hybrid systems [2] so they are key components in several sectors. For instance, SCs are good options to overcome one of the drawbacks of renewable energy sources, intermittent power production [3]. As part of regenerative power systems, SCs play an essential role in the improvement of the efficiency of automotive and land transportation sectors systems [4]. Even in space missions, this technology can improve the capabilities of small satellites, making it possible for them to operate high-power payloads [5]. The potential of SCs can be exploited with their combination with other storage technologies (e.g., batteries, fuel cells, etc.). In these hybrid systems, there is a trade-off between the energy stored, peak power capabilities, cost, design, maintenance, and operation complexity and reliability.

The performance of SCs is between that of traditional capacitors and electrochemical batteries. The energy density of modern SCs is between 3 and 6 orders of magnitude higher than that of capacitors [6], but 1-3 lower than that of batteries [6], [7]. However, they can be charged and discharged quickly, being their specific power between 2 and 3 orders of magnitude larger than batteries [7]. This makes SCs perfect devices for applications in which a large amount of energy must be delivered or stored in a short period of time. SCs have more advantages, as they have higher efficiencies due to their very low equivalent series resistance (ESR) [8]. Furthermore, they can withstand

The associate editor coordinating the review of this manuscript and approving it for publication was Ching-Ming Lai.

millions of full charge-discharge cycles, not as in the case of batteries whose life is limited to many thousands of cycles with a limited Depth of Discharge (DoD) [9]. Additionally, SCs are less sensitive to temperature changes and can provide energy at very low temperatures when compared with batteries [6]. The main drawback of SCs is their low rating voltages, being needed many SCs connected in series and power converters to supply power at an appropriate voltage level. In addition, SCs present high self-discharge rates, so they are not suitable for long-term energy storage. Another disadvantage is their limited frequency response. In particular, capacitance is neglected for medium and high-frequency charging/discharging applications, so SCs become useless in AC applications. Even in DC applications, filter circuits are needed to reduce the adverse effects of the AC components.

The implementation of an effective mathematical model of SCs is key to predict their performance and the adverse effects produced, in particular, during transient by non-linear loads. In addition, it plays a crucial role in optimising the power system design and setting the best power management strategies. Many models are reported in the literature; still, the selection of the most suitable one has to be made according to the application, the stage of the design, and the available resources. According to Zhang et al. [10], the most commonly used models to simulate the electrical behaviour of SCs are the electrochemical, equivalent circuit, fractional order and intelligent (artificial neural network and fuzzy logic) models. Indeed, there is a trade-off between accuracy, calculation efficiency and required data. In the case of equivalent circuit models, such three parameters are balanced as a relatively small amount of data, obtained from electrical tests, is required to predict accurately the response of SCs in real-time simulations.

The simplest equivalent circuit models, shown in Fig. 1, have been used in previous works [11], [12], [13] to describe the overall behaviour of SCs. The model in Fig. 1(a) is composed of a capacitance, C, and an equivalent series resistance, ESR. Regarding the model in Fig. 1(b), an equivalent parallel resistance, EPR, is connected in parallel to the capacitance to take into account the long-term self-discharging losses. These two equivalent circuits are useful for the initial sizing of power systems, and even for simulating low-rate and stationary charging and discharging processes. Moreover, the implementation of these equivalent circuits is easy, as their parameters can be extracted directly from the manufacturer's datasheet.

The circuits can also be modified to include the capacitance variation with the SCs' voltage. With this simple modification, the stationary response of SCs is more accurate than in previous models at the expense of requiring experimental data to obtain an empirical function of the capacitance, $c(v)$, in terms of the voltage across the capacitor, v.

In addition, there are several complex models, the so-called multibranch models, that can emulate both the stationary and

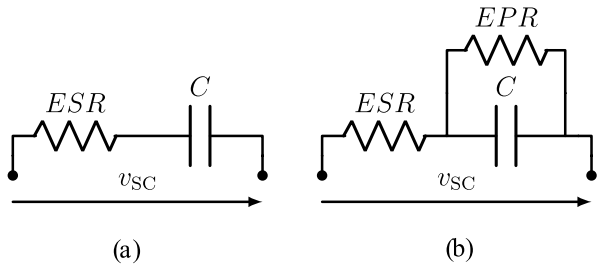

FIGURE 1. Simple models of SCs: (a) simple model with ESR (b) simple model with EPR.

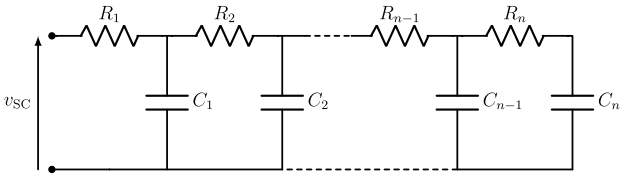

FIGURE 2. Transmission line model of SCs.

the dynamic response of SCs with high accuracy. A well-known example is the transmission line model, shown in Fig. 2, which is composed of several resistors and variable capacitors. The time constants associated to the RC branches are able to reproduce with a high fidelity the redistribution and the self-discharge phenomenon. A different multibranch model, composed of several parallel branches (see Fig. 3), was proposed in [14]. A non-stationary version of this widely used model, requiring three parallel branches, was introduced in [15]. Two of these branches are composed of one resistor in series with one capacitor, whereas the third branch consists of one resistor and is responsible for modelling the self-discharge phenomena. All parameters, except the capacitor of the main branch, have constant values. Finally, a more accurate non-stationary model presented in [16] is a parallel model in which the main branch has one resistor and one variable capacitor in series with several variable resistors and capacitors in parallel (see Fig. 4). These multibranch circuits have been reported to be very accurate [14], [16], [17], as they can model three of the most important phenomena that affect SC performance: the voltage level, frequency, and self-discharge. However, obtaining all the required parameters of these models is not an easy task, several dynamic tests and costly and complex simulations being required, as described in [18].

Many procedures have been proposed in the literature to obtain model parameters, varying in implementation complexity and accuracy. The most straightforward procedures are based on estimating the model parameters after performing experimental tests. On the contrary, online identification methods require a more complex experimental setup, as measured data must be processed in real-time, and the algorithms to be implemented are also complicated.

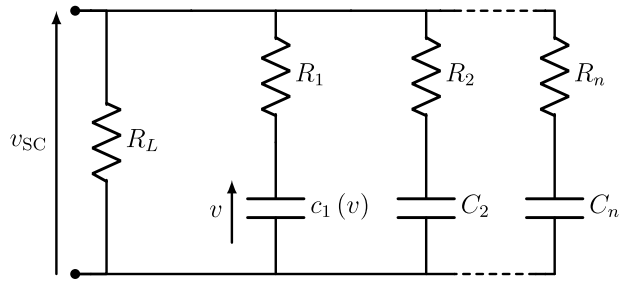

FIGURE 3. Parallel model of SCs.

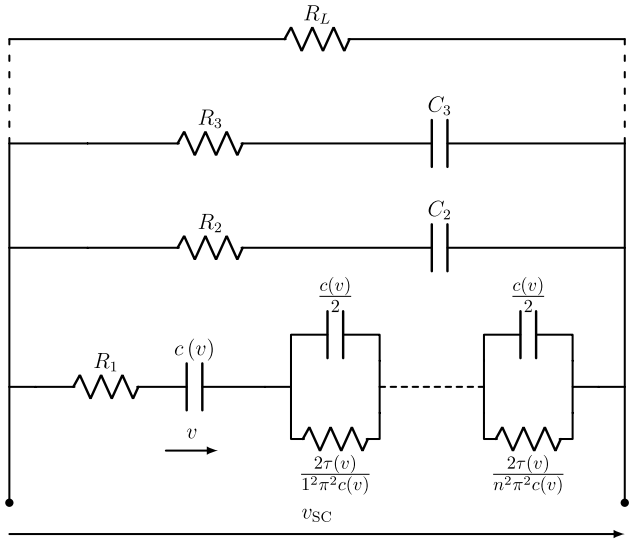

FIGURE 4. Extended parallel model of SCs.

Regarding the post-processing procedures, the ones based on circuit analysis are well-extended. For example, in [14] and [15] simple analytic expressions are formulated to extract the model parameters from a few experimental data points from a charging test. In this approach, each branch can be analysed independently, as a different order of magnitude in the time constants of each branch is considered. In addition, other procedures are based on minimising some error parameters, such as the sum squared error [18], [19], when comparing experimental data with simulation results.

As regards to online methods, the recursive least square method [20], [21], the unscented Kalman filter [22], the Weighting bat algorithm [23] and the Luenberger-style technique [24] have been implemented to identify the parameters of the SC model.

All the above mentioned procedures, excluding the circuit analysis, share the same problem. As in many optimisation problems, in order to improve the convergence speed, it is fundamental not only to implement an appropriate algorithm but also to provide initial values for the parameters to be optimised. Then, it is necessary to determine a method to provide accurate initial values.

The aim of this paper is to describe a new procedure to speed up the identification of the electrical parameters of a well-known SC model. The novel contribution of the paper consists of the combined use of the basic information, extracted by means of just one electrical test, and specific analytical procedure applied to the parameters identification of the one- and two-branches models.

This paper is organised as follows: Section II introduces the equivalent circuits of SC used in this work: the one and two-branches models. Section III describes a new methodology for estimating the electrical parameters of the two-branches model. This methodology and also the accuracy of the two-branches model are validated with experimental data, the results being included in Section IV. Finally, the conclusions are summarised in Section V.

II. ONE AND TWO-BRANCHES MODELS

The one and two-branches models are the equivalent electrical circuits used in this work, as shown in Fig. 5. The former is utilised to obtain a first estimation of the parameters of the latter. The two-branches model is a simplification of the parallel model proposed in [15] (see Fig. 5 (b)). This simplification consists of removing the leakage resistor, R_L, as it makes it easier to calculate the rest of the parameters. Note that the self-discharging effect on SCs is negligible in short- and mid-term simulations. Nevertheless, readers interested in including this phenomenon can take an initial value of R_L from the SC datasheet and then optimise it with the rest of the parameters.

Even though the two-branches model may seem too simple, it has been reported a good match between experimental and simulated data. In fact, it is widely used for global energy management [25], [26], [27], [28]. The good accuracy of this model is demonstrated in Section IV even in the case of variable environmental and operating conditions. As mentioned above, the thermal stability of SCs makes them behave similarly even in a wide range of operating temperatures. For example, constant charging and discharging tests performed at temperatures between -40 °C and 20 °C in [29] and -20 °C and 40 °C in [30] reported a maximum deviation, in relation to the extreme temperatures, of ≈ 40 mV in the measured voltage. Instead, the maximum deviation in the measured voltage between more realistic operating temperatures is negligible in both studies. Then, an electrothermal characterisation of an SC may be required only in power applications under wide thermal variability.

III. METHOD DESCRIPTION

The proposed methodology to model the SC starts by performing a simple test. The SC is discharged at a constant current, starting from its rated voltage, V_0, and ending at half of its rated voltage, when the remaining energy has dropped approximately 75%. The discharging profile (voltage vs. time) is then analysed with easy numerical techniques to extract some valuable information. With these data, an iterative procedure to obtain the main electrical

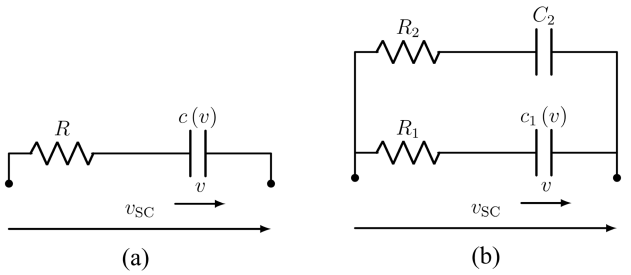

FIGURE 5. Models used in the current paper: (a) one-branch model and (b) two-branches model.

parameters of the SC begins. First, the behaviour of the SC is modelled with one of the most basic equivalent circuits (here called the one-branch model). The parameters of the model are estimated based on comparing a fitting function of the experimental data with the analytical solution of the model and the energy balance equation. Then, these parameters are used as initial guesses to apply the least squares method (LSM) so that the optimal parameters of the model can be found. In the second place, a more representative model of the SC (here called the two-branches model) is used. To identify the electrical parameters of this model, some data of the transient and quasi-stationary parts of the discharging curve are compared against the analytical frequency response of the model. The new parameters are then used as an initial guess to implement the last LSM to optimise the model parameters. A summary diagram of the step-by-step procedure is included in Fig. 6.

A. ONE-BRANCH MODEL

This model consists of one-branch composed of one resistor and one capacitor (see Fig. 5(a)). The SC voltage, v_{SC}, is calculated with (1), where v, I and R are the internal voltage, the discharge current (defined as positive) and the internal resistance, respectively.

$$v_{SC} = v - IR. \tag{1}$$

The current and the resistance are supposed as constant parameters, so v_{SC} is determined after solving v. This is carried out by solving the governing equation of the SC:

$$I = -\frac{dq}{dt}, \tag{2}$$

where q is the charge of the capacitor, defined from the capacitance, $c\,(v)$ and the internal voltage of the SC, v, as:

$$q = c\,(v)\,v, \tag{3}$$

$$c\,(v) = C_0 + Kv. \tag{4}$$

Substituting the expression of $c\,(v)$ (see (4)) into (3) and taking the derivative of q, the governing equation of the supercapacitor (see (2)) can be rewritten as follows:

$$I = -\,(C_0 + 2Kv)\,\frac{dv}{dt}. \tag{5}$$

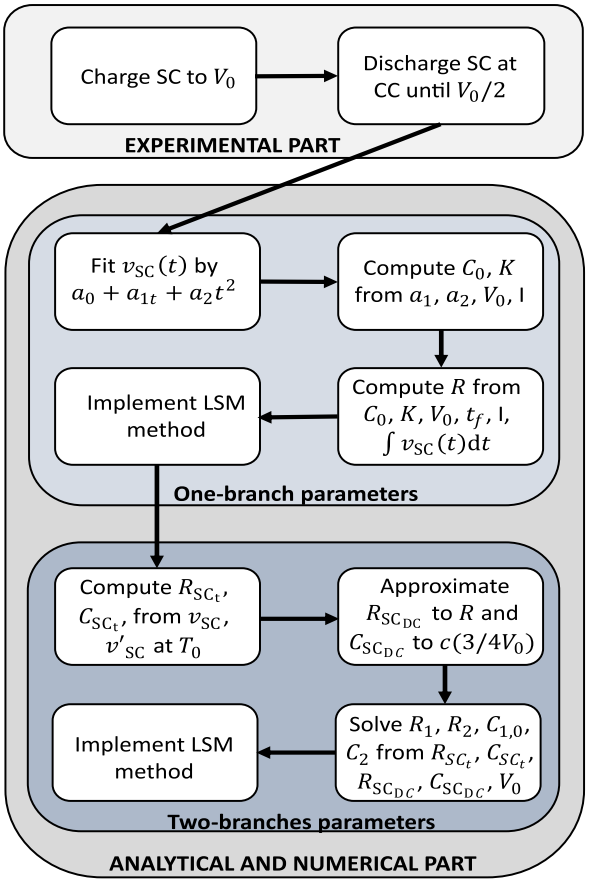

FIGURE 6. Summary diagram of the proposed parameter identification procedure.

As mentioned above, the discharge current, I, is assumed to be constant. Then, the governing differential equation has the following analytical solution:

$$v\,(t) = \frac{-C_0 + \sqrt{(C_0 + 2KV_0)^2 - 4KI\,(t - T_0)}}{2K}, \tag{6}$$

where V_0 is the internal voltage at the beginning of the test ($T_0 = 0$ s).

According to the experimental tests shown in [31] and based on previously published works, the steady response of v_{SC} can be approximated by a low-degree polynomial function. For this method, it is required, at least, a second-order polynomial function. Let f be a quadratic fitting function of the steady response of the experimental voltage curve v_{SC}, defined by coefficients a_0, a_1 and a_2 (see (7) and (8)). This approximation is very accurate during the steady response part, but cannot reproduce the exponential decay associated to the transient response. However, this approximation is satisfactory to extract some useful data. As R and I are constant, the first derivative of the SC voltage, $v_{SC}{}'$, coincides with the first derivative of its internal voltage, v', (see (9)). Then, v' can be approximated by the first

derivative of f, f':

$$v_{SC} \approx f(t), \tag{7}$$
$$f(t) = a_0 + a_1 t + a_2 t^2, \tag{8}$$
$$v_{SC}{}' = v', \tag{9}$$
$$v' \approx f'. \tag{10}$$

Developing the Taylor series of v' at the origin and retaining only the linear contribution, the parameters C_0 and K can be related with the coefficients a_0, a_1 and a_2. Let v' be approximated by:

$$v'(t) \approx v'(0) + v''(0)\, t, \tag{11}$$

where $v'(0)$ and $v''(0)$ are obtained from the first and second derivatives of (6):

$$v'(0) = -\frac{I}{C_0 + 2KV_0}, \tag{12}$$
$$v''(0) = -\frac{2KI^2}{(C_0 + 2KV_0)^3}, \tag{13}$$

and are related to the coefficients of function f as:

$$v'(0) = a_1, \tag{14}$$
$$v''(0) = 2a_2. \tag{15}$$

Then, C_0 and K can be identified as:

$$C_0 = -\frac{I}{a_1}\left(1 + \frac{2V_0 a_2}{a_1^2}\right), \tag{16}$$
$$K = \frac{a_2 I}{a_1^3}. \tag{17}$$

Finally, using the energy conservation equation applied to a complete discharge test during a fixed time interval, T_f, the internal resistance of the SC can be found:

$$\Delta E_{SC} = E_t + \int_{T_0}^{T_f} RI^2 \mathrm{d}t. \tag{18}$$

On the left side of (18), ΔE_{SC} is the total energy supplied by the SC:

$$\Delta E_{SC} = -\int_{Q_0}^{Q_f} v \mathrm{d}q, \tag{19}$$

where Q_0 and Q_f are the charge of the SC at the beginning and the end of the discharge test, respectively. The integral of (19) can be redefined in terms of capacitance and voltage (see (2) and (5)) as:

$$\Delta E_{SC} = -\int_{V_0}^{V_f} (C_0 + 2Kv)\, v \mathrm{d}v. \tag{20}$$

After performing the integral of (20), ΔE_{SC} can be expressed as follows:

$$\Delta E_{SC} = \frac{1}{2}C_0\left(V_0^2 - V_f^2\right) + \frac{2}{3}K\left(V_0^3 - V_f^3\right), \tag{21}$$

where V_f is the internal voltage at the end of the discharge test and can be approximated, particularising (6) at $t = T_f$.

Regarding the right side of (18), the first term, E_t, represents the energy consumed by the external load during the test. It is calculated numerically from the experimental data and is defined as:

$$E_t = \int_{T_0}^{T_f} v_{SC} I \mathrm{d}t. \tag{22}$$

Also, the second integral accounts for the ohmic losses and can be simplified as follows:

$$\int_{T_0}^{T_f} RI^2 \mathrm{d}t = RI^2 T_f. \tag{23}$$

Finally, R is solved as:

$$R = \frac{\Delta E_{SC} - E_t}{I^2 T_f}. \tag{24}$$

B. TWO-BRANCHES MODEL

This model consists of two parallel branches composed of one resistor and one capacitor each as illustrated in Fig. 5(b). This model improves the transient response of the previous model without significantly increasing the complexity of the model. The main branch is characterised by resistance R_1 and capacitance $c_1(v_1)$. These parameters have the same order of magnitude as the respective ones of the one-branch model. In addition, $c_1(v_1)$ has a linear voltage dependence:

$$c_1(v_1) = C_{1,0} + K_1 v_1, \tag{25}$$

where v_1 is the voltage of the capacitor of the main branch, $C_{1,0}$ is its capacitance when fully discharged, and K_1 is the slope. Regarding the second branch, the resistance R_2 and the capacitance C_2 are constant and determine the dynamic response of the SC.

The analysis of the circuit in the frequency domain leads to a preliminary estimation of the circuit parameters. The equivalent impedance of the SC is given by:

$$z_{SC}(\omega) = r_{SC}(\omega) + j x_{SC}(\omega), \tag{26}$$

where r_{SC} and x_{SC} are the resistance and reactance components defined as:

$$r_{SC}(\omega) = \frac{(\omega c_1 C_2)^2 R_1 R_2 (R_1 + R_2) + c_1^2 R_1 + C_2^2 R_2}{(\omega c_1 C_2 (R_1 + R_2))^2 + (c_1 + C_2)^2}, \tag{27}$$

$$x_{SC}(\omega) = \frac{(c_1 + C_2)\left(\omega^2 R_1 R_2 c_1 C_2 - 1\right)}{(\omega c_1 C_2 (R_1 + R_2))^2 + (c_1 + C_2)^2} - \frac{\omega^2 c_1 C_2 (c_1 R_1 + C_2 R_2)(R_1 + R_2)}{(\omega c_1 C_2 (R_1 + R_2))^2 + (c_1 + C_2)^2}. \tag{28}$$

The equivalent capacitance of the SC, c_{SC}, is given by:

$$c_{SC}(\omega) = -\frac{1}{\omega x_{SC}}, \tag{29}$$

and the substitution of x_{SC} of (28) leads to the following expression:

$$c_{SC}(\omega) = \frac{(\omega c_1 C_2 (R_1 + R_2))^2 + (c_1 + C_2)^2}{\omega^2 c_1 C_2 \left(c_1 R_1^2 + C_2 R_2^2\right) + (c_1 + C_2)}. \tag{30}$$

Under DC conditions, the equivalent resistance and capacitance of the SC, $R_{SC_{DC}}$ and $C_{SC_{DC}}$, are given by (31) and (32), respectively. Regarding fast transients ($\omega \to \infty$), the equivalent resistance and capacitance, R_{SC_t} and C_{SC_t}, are obtained with (33) and (34), respectively. Note that in this approach c_1 has to be particularised to obtain $R_{SC_{DC}}$, R_{SC_t}, and C_{SC_t}:

$$R_{SC_{DC}} = \frac{c_1^2 R_1 + C_2^2 R_2}{(c_1 + C_2)^2}, \tag{31}$$

$$C_{SC_{DC}} = c_1 + C_2, \tag{32}$$

$$R_{SC_t} = \frac{R_1 R_2}{R_1 + R_2}, \tag{33}$$

$$C_{SC_t} = \frac{c_1 C_2 (R_1 + R_2)^2}{R_1^2 c_1 + R_2^2 C_2}. \tag{34}$$

At the beginning of the discharging process, there is a fast transient so R_{SC_t} can be approximated knowing the initial voltage drop (see (35)). Similarly, C_{SC_t} can be approximated by the first derivative of v_{SC} (see (36)). On the other hand, after the transient, the low dynamics of the model cause the SC to behave in a quasistatic manner and can be modelled with $R_{SC_{DC}}$ and $C_{SC_{DC}}$. In particular, $R_{SC_{DC}}$ can be approximated by the resistance obtained from the one-branch model and $C_{SC_{DC}}$ is bounded by the minimum and maximum capacitance of $c(v)$ from the one-branch model. An initial guess of $C_{SC_{DC}}$ could be the corresponding $c(v)$ in the middle of the discharge process (see (37) and (38)). Considering that a typical discharge ends when the SC voltage drops to its half voltage rate, $V_0/2$, $v = 3/4V_0$ is chosen. Then, as a first approximation of $R_{SC_{DC}}$, $C_{SC_{DC}}$, R_{SC_t}, and C_{SC_t} is known, the system of equations (31)-(34) can be solved:

$$R_{SC_t} = \frac{V_0 - v_{SC}(0)}{I}, \tag{35}$$

$$C_{SC_t} = -\frac{I}{v_{SC}'(0)}, \tag{36}$$

$$R_{SC_{DC}} \approx R, \tag{37}$$

$$C_{SC_{DC}} \approx c\left(\frac{3}{4}V_0\right). \tag{38}$$

Once c_1 (v_1) is solved for a particular v_1 ($v_1 = v = 3/4V_0$), K_1 can be approximated to K of the one-branch model, so $C_{1,0}$ can be calculated as follows:

$$C_{1,0} = c_1 - K\frac{3}{4}V_0. \tag{39}$$

Finally, as in the case of the one-branch model, the final identification of $C_{1,0}$, K_1, R_1, C_2 and R_2 can be done by implementing another LSM, considering the initial guess of these parameters the ones estimated with the explained methodology. However, in this case, it is crucial to use the full discharge data of the SC, as the transient is relevant to obtain reasonable values of C_2 and R_2. For this procedure, the two-branches model can be solved numerically. The differential equation system is described in the Appendix .

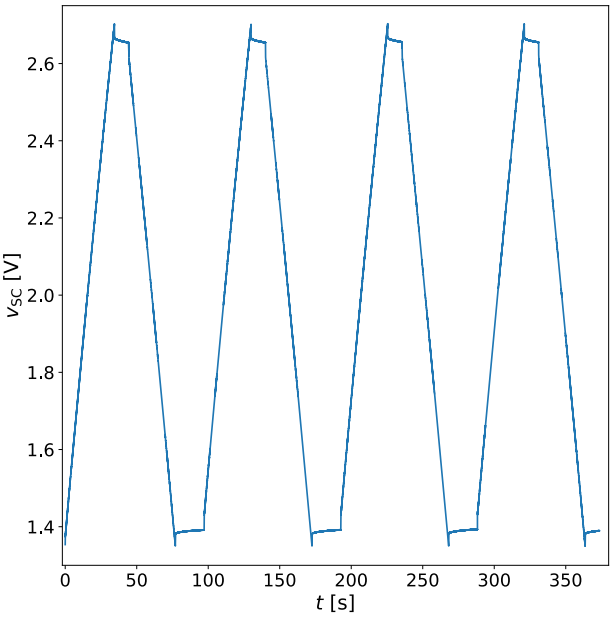

FIGURE 7. Voltage evolution of the 2.7 V 3000 F Maxwell SC during four charge-discharge cycles test at 120 A constant current [31].

IV. EXPERIMENTAL VALIDATION

The experimental data published in [31] have been used to: 1) study the potential of the iterative methodology, explained in the previous section, to identify the parameters of the two-branches model and 2) check the accuracy of the two-branches model in long-term simulations.

Among all the tests carried out on [31], the authors have considered the data (i.e., current and voltage vs. time) of charge-discharge cycles of a 2.7 V 3000 F Maxwell SC [32] at different constant current rates. In particular, the data of the charge-discharge cycles at 120 A constant current (see Fig. 7) have been used to identify the model parameters.

The parameters of the one-branch model have been obtained with the methodology explained in this paper. The steady part of the first discharge cycle has been fitted (see Fig. 8) with a second-order polynomial function whose parameters (a_0, a_1, and a_2) are listed in Table 1. The coefficients of the linear capacitance, C_0 and K, have been obtained from a_1 and a_2 by (16) and (17). To estimate the resistance, R, (24) has been applied considering that the total energy supplied by the SC, ΔE_{SC}, and the energy consumed by the external load, E_t, have been calculated with (21) and (22) (analytically and numerically, respectively). For the calculation of E_t, a fully charged SC has been assumed at the beginning ($V_0 \approx 2.65$ V) and V_f has been calculated with (6) considering a discharge time of approximately 32.6 s. The parameters of the one-branch model calculated with this procedure and the ones obtained by LSM are illustrated in Table 2. The relative errors of C_0, and R are very low (-1.97%, and -2.47%, respectively), and except for the relative error of K (11.58%), the approximation shows good results.

TABLE 1. Parameters required for the estimation of the electrical parameters of the one-branch model.

a_0 [V]	a_1 [mVs^{-1}]	a_2 [μVs^{-2}]	T_f [s]	V_f [V]	ΔE_{SC} [kJ]	E_t [kJ]
2.62	−37.34	−45.51	32.61	1.38	8.03	7.88

TABLE 2. Electrical parameters of the one-branch model.

	C_0 [F]	K [F/V]	R [mΩ]
Proposed method	2688	106	0.315
LSM	2742	95	0.323

TABLE 3. Parameters required for the estimation of the electrical parameters of the two-branches model.

R_{SC_t} [mΩ]	$R_{SC_{DC}}$ [mΩ]	C_{SC_t} [F]	$C_{SC_{DC}}$ [F]
0.224	0.315	861	2899

TABLE 4. Electrical parameters of the two-branches model.

	$C_{1,0}$ [F]	K_1 [F/V]	R_1 [mΩ]	C_2 [F]	R_2 [mΩ]
R. Faranda [15]	2098	248	0.182	483	23.21
Proposed method	2570	95	0.341	118	0.649
LSM	2616	98	0.349	114	0.666

The parameters of the two-branches model have been calculated by analysing the transient and the steady responses of the discharge curve as explained in the previous section. The resistance and capacitance during the transient state, R_{SC_t} and C_{SC_t}, have been approximated with the voltage drop and voltage derivative during the first milliseconds of the test (see (35) and (36)). The steady-state parameters, $R_{SC_{DC}}$ and $C_{SC_{DC}}$, have been selected from the one-branch model (see (37), (38) and (39)). These parameters are presented in Table 3. With these parameters, together with the system of equations (31)-(34), the parameters of the two-branches model have been estimated. In Table 4 the parameters of the two-branches model estimated with this procedure and the optimised ones with a LSM are shown. The relative errors of both the parameters of the first branch $C_{1,0}$, K_1, and R_1 (−1.76%, −3.06% and −2.29%, respectively) and the ones of the second branch C_2 and R_2 (3.51% and −2.55%, respectively) are low, so the proposed methodology allows a fast-converging LSM. These promising results are not in line with those obtained with the procedure developed by R. Faranda in [15] (see Table 4). In this case, large relative errors with reference to the optimised results of the LSM have been found. In particular, the relative errors of parameters $C_{1,0}$, K_1, R_1, C_2 and R_2 are −19.8%, 153%, −47.9%, 324% and 3385%, respectively.

The two-branches model has been implemented in Simulink with the optimum parameters listed in Table 4. Then, the complete cycle tests (80 A, 90 A, 100 A, 110 A. 120 A and 130 A) have been simulated. In Fig. 9 the voltage evolution of the SC as a function of time for each test is shown. Also, the absolute error of the model with respect to

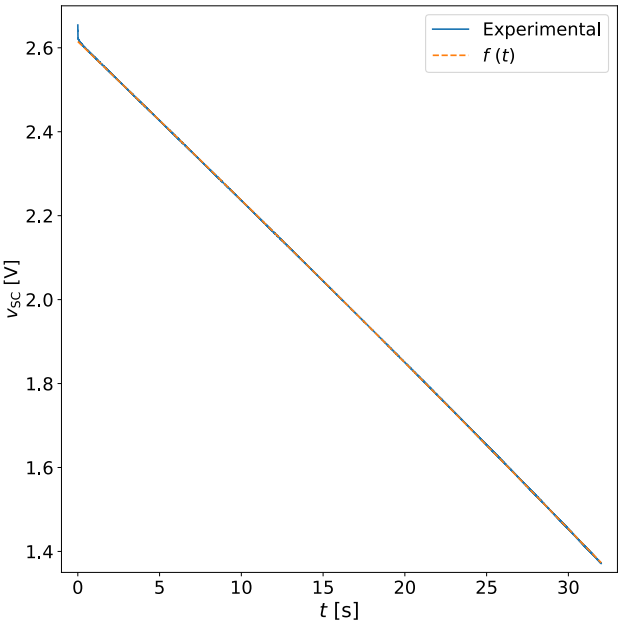

FIGURE 8. Comparison of the first discharging cycling [31] and approximated one by second-order polynomial function $f(t)$.

TABLE 5. Absolute and relative errors between the experimental data [31] and the simulated results during six constant current charge-discharge cycles. The maximum, mean and standard deviation of the absolute errors are E_{max}, $\overline{E}$ and σ_E, whilst the corresponding relative errors are e_{max}, $\overline{e}$, and σ_e.

I [A]	E_{max} [mV]	$\overline{E}$ [mV]	σ_E [mV]	e_{max} [%]	$\overline{e}$ [%]	σ_e [%]
80	170.21	77.89	46.95	11.70	3.98	2.62
90	52.49	10.77	8.77	3.45	0.56	0.58
100	78.65	13.15	14.15	4.91	0.67	0.69
110	97.16	24.98	22.59	6.06	1.25	1.17
120	117.09	25.84	29.92	7.53	1.39	1.72
130	139.48	35.76	38.66	9.14	1.75	1.89

the experimental data is plotted. The evolution of the relative error is shown in Fig. 10. In addition, a summary of the absolute and relative errors of the model are included in Table 5.

According to these results, the maximum deviations between the model and the experimental data occur during transients, when a charge or discharge cycle ends and a 10 seconds rest starts, or vice versa. In all cases, except for the 80 and 90 A cases, both the absolute and relative error have a clear tendency in the error increase. Also, in these cases (100 A - 130 A) the errors are in the same order of magnitude from the beginning. In contrast, the errors of the most accurate simulation (see Fig. 11), the 90 A case, do not have a clear tendency, as they start increasing and then decreasing. Finally, in the less accurate simulation (see Fig. 11), the 80 A case, the deviations in the first and second cycles are between 2 and 4 orders of magnitude higher than the rest of the cases, and then they stabilise.

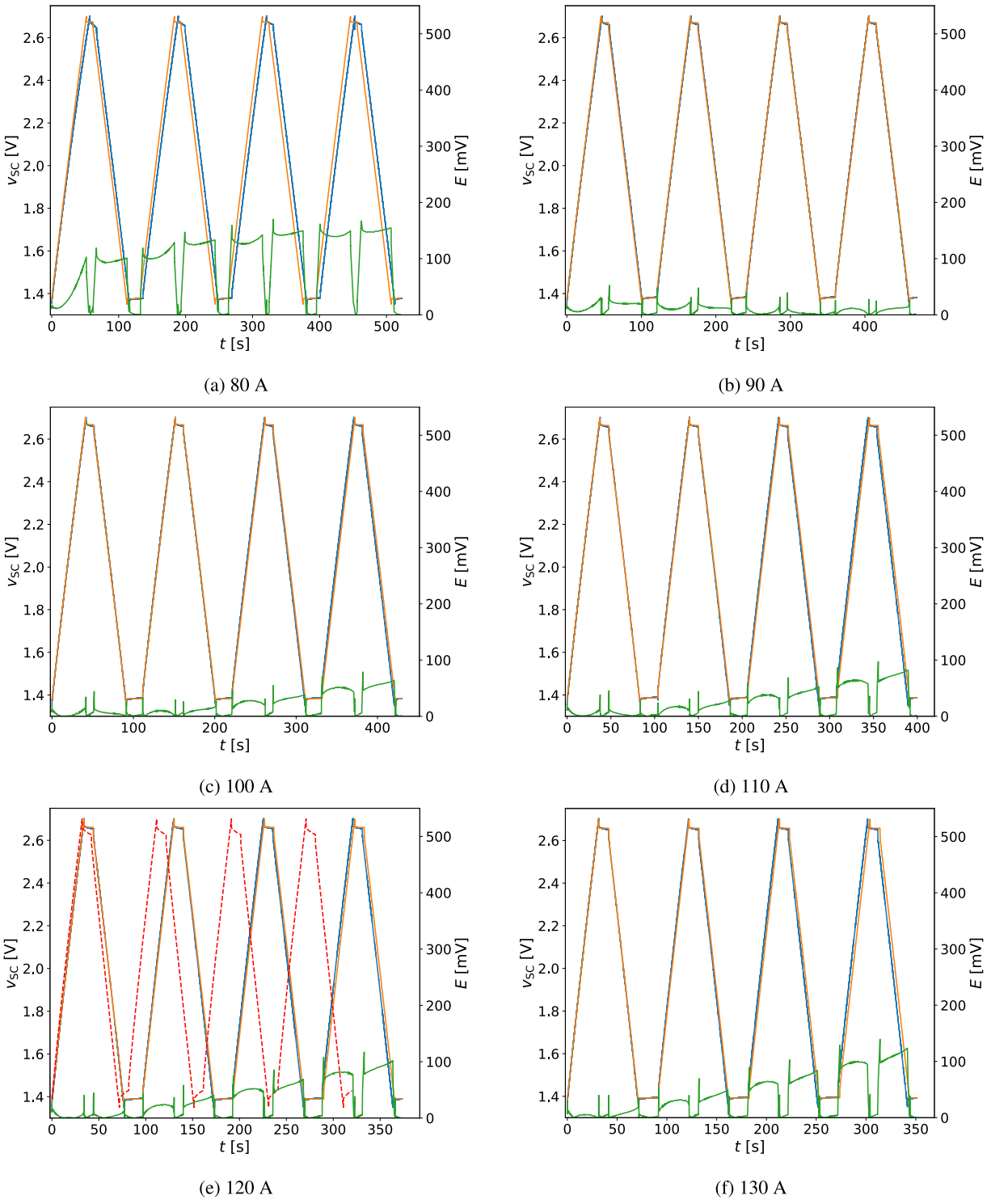

FIGURE 9. Time evolution of the 2.7 V 3000 F Maxwell SC voltage, v_{SC}, and absolute error, E, between the experimental data [31] and the simulation during four charge-discharge cycles at different constant currents. The blue and the orange lines (left axis) represent the measurements and the simulated data, respectively, and the green lines represent the absolute error (right axis). The red dashed line of (e) indicates the voltage simulated with the parameters obtained with [15].

It should be remarked that, paradoxically, the 120 A simulation case (the one in which the parameters of the model have been optimised), does not present the minimum value of the mean relative error. However, according to the results, the two-branches model is capable of predicting with high accuracy, except during the transients, the voltage evolution

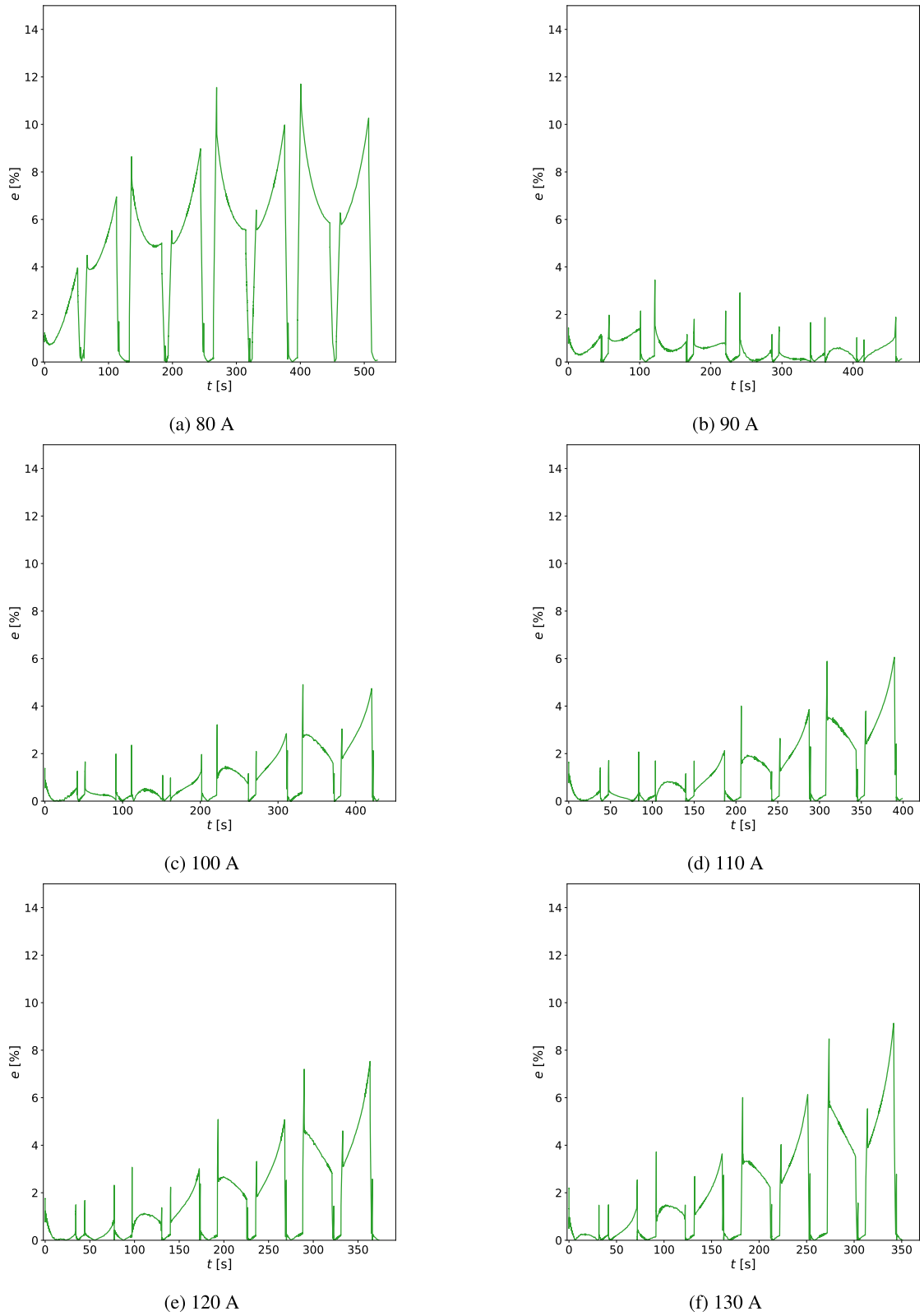

(a) 80 A (b) 90 A

(c) 100 A (d) 110 A

(e) 120 A (f) 130 A

FIGURE 10. Time evolution of the relative error, *e*, of the 2.7 V 3000 F Maxwell SC voltage, between the experimental data [31] and the simulation during four charge-discharge cycles at different constant currents.

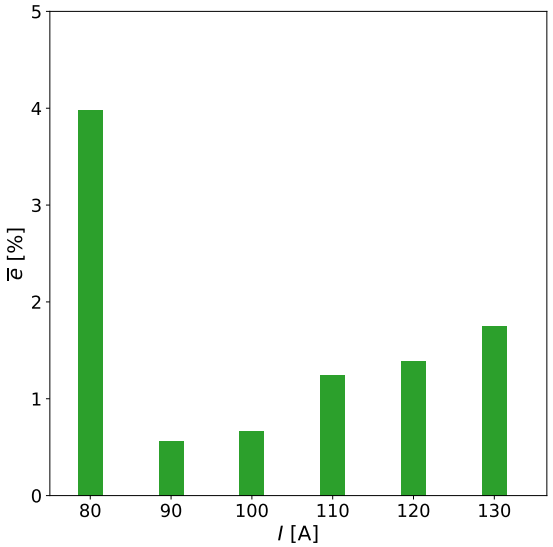

FIGURE 11. Mean relative error, $\bar{e}$, of the 2.7 V 3000 F Maxwell SC voltage between the experimental data [31] and the simulation during four charge-discharge cycles at different constant currents.

of the SC under charge and discharge cycles at different constant currents.

In order to compare the results produced by the proposed procedure with the ones obtained using the parameters' values estimated by method [15], the 120 A cycle test has been simulated. According to these results, shown in Figure 9e, the procedure proposed in [15] is accurate only during short-time simulations. After the first charging and discharging cycle, the voltage deviation grows rapidly.

The promising results obtained with the proposed method should be considered in light of some limitations. First, the self-discharge phenomenon has been neglected, thus the accuracy of the two-branches model suffers over long periods of inactivity or during charge-discharge processes at very low currents. Even for the charge-discharge cycles at high constant currents analysed in this work, the error of the two-branches model, except for the 90 A case, has a clear increasing tendency and is presumably related to the self-discharge. The second limitation, common to most procedures, concerns the assumption of high thermal stability of the SC. For extreme environmental temperature variations, the model results could deviate excessively from the real data.

All of these limitations suggest the following directions for future research:

- The two-branches model should incorporate a variable leakage resistor. Then, the parameter identification method must be restricted to high discharging currents so the self-discharge branch can be ignored as the leakage current is negligible. However, to determine the variable leakage resistor, an additional electrical test and parameter identification method must be included.
- The electrical tests should be performed at different environmental temperatures (given by the real application of the SC) in order to analyse the temperature dependence of the model parameters. Those parameters with high-temperature variation should be modelled with simple temperature-dependent functions.

V. CONCLUSION

The data of just one discharge test at constant current has been successfully employed to extract useful data to model the one and the two-branches models of the SC. The proposed procedure is useful for estimating the parameters of a one- and two-branches SC model. As the proposed methodology provides initial estimated values close enough to the optimised parameters, the LSM requires a low number of iterations and computational time. The two-branches model selected to simulate the SC describes with good precision the behaviour of an SC under constant current charge/discharge cycles in a wide current range. Additionally, the easy procedure and the simple and quick discharge test, make it easy to implement high-precision simulations in an SC model. Further investigations should focus on improving the estimation procedure to be implemented on a more precise model that emulates the self-discharge phenomenon and the thermal behaviour of SCs.

APPENDIX A
EQUATIONS OF THE TWO-BRANCHES MODEL OF SC

According to the circuit depicted in Fig. 5(b), the output voltage of the SC is given by the following equation:

$$v_{SC} = v_1 + \left(C_{1,0} + K_1 v_1\right) v_1' R_1, \tag{40}$$

where v_1 is the internal voltage of c_1 and the terms multiplying R_1 correspond to the net charging current of c_1. The unknown function v_1 has to be solved in order to obtain the output voltage of the SC. For this undertaking, the following system of differential equations 41, together with the initial conditions of (42), is solved:

$$\begin{bmatrix} v_1' \\ v_2' \end{bmatrix} = \begin{bmatrix} -a & a \\ b & -b \end{bmatrix} \begin{bmatrix} v_1 \\ v_2 \end{bmatrix} + \begin{bmatrix} c \\ d \end{bmatrix}, \tag{41}$$

$$\begin{bmatrix} v_1(0) \\ v_2(0) \end{bmatrix} = \begin{bmatrix} V_0 \\ V_0 \end{bmatrix}, \tag{42}$$

where v_2 is the internal voltage of C_2, V_0 is the voltage of the SC at the beginning of the simulation and a, b, c, and d are defined as:

$$a = \frac{1}{\left(C_{1,0} + 2K_1 v_1\right)\left(R_1 + R_2\right)}, \tag{43}$$

$$b = \frac{1}{C_2\left(R_1 + R_2\right)}, \tag{44}$$

$$c = aR_2 I, \tag{45}$$

$$d = bR_1 I. \tag{46}$$

ACKNOWLEDGMENT

The authors would like to thank Antonio Morandi and Alessandro Lampasi for providing experimental data. The

author Sergio Marín-Coca thanks the Department of Industrial Engineering of the University of Rome "Tor Vergata" for allowing him to conduct this research at its facilities.

REFERENCES

[1] J. Zhao and A. F. Burke, "Electrochemical capacitors: Performance metrics and evaluation by testing and analysis," *Adv. Energy Mater.*, vol. 11, no. 1, Jan. 2021, Art. no. 2002192.

[2] J. F. Pedrayes, M. G. Melero, J. M. Cano, J. G. Norniella, S. B. Duque, C. H. Rojas, and G. A. Orcajo, "Lambert W function based closed-form expressions of supercapacitor electrical variables in constant power applications," *Energy*, vol. 218, Mar. 2021, Art. no. 119364.

[3] A. González, E. Goikolea, J. A. Barrena, and R. Mysyk, "Review on supercapacitors: Technologies and materials," *Renew. Sustain. Energy Rev.*, vol. 58, pp. 1189–1206, May 2016.

[4] Z. Zou, J. Cao, B. Cao, and W. Chen, "Evaluation strategy of regenerative braking energy for supercapacitor vehicle," *ISA Trans.*, vol. 55, pp. 234–240, Mar. 2015.

[5] T. Shimizu and C. Underwood, "Super-capacitor energy storage for micro-satellites: Feasibility and potential mission applications," *Acta Astronautica*, vol. 85, pp. 138–154, Apr. 2013.

[6] M. Şahin, F. Blaabjerg, and A. Sangwongwanich, "A comprehensive review on supercapacitor applications and developments," *Energies*, vol. 15, no. 3, p. 674, Jan. 2022.

[7] J. R. Miller and P. Simon, "Electrochemical capacitors for energy management," *Science*, vol. 321, no. 5889, pp. 651–652, Aug. 2008.

[8] G. G. Prasad, N. Shetty, S. Thakur, and K. B. Bommegowda, "Supercapacitor technology and its applications: A review," *IOP Conf. Ser., Mater. Sci. Eng.*, vol. 561, no. 1, Oct. 2019, Art. no. 012105.

[9] G. Ning and B. N. Popov, "Cycle life modeling of lithium-ion batteries," *J. Electrochem. Soc.*, vol. 151, no. 10, p. A1584, 2004.

[10] L. Zhang, X. Hu, Z. Wang, F. Sun, and D. Dorrell, "A review of supercapacitor modeling, estimation, and applications: A control/management perspective," *Renew. Sustain. Energy Rev.*, vol. 81, no. 2, pp. 1868–1878, Jan. 2018.

[11] D. Linzen, S. Buller, E. Karden, and R. W. De Doncker, "Analysis and evaluation of charge-balancing circuits on performance, reliability, and lifetime of supercapacitor systems," *IEEE Trans. Ind. Appl.*, vol. 41, no. 5, pp. 1135–1141, Sep./Oct. 2005.

[12] R. L. Spyker and R. M. Nelms, "Classical equivalent circuit parameters for a double-layer capacitor," *IEEE Trans. Aerosp. Electron. Syst.*, vol. 36, no. 3, pp. 829–836, Jul. 2000.

[13] B. E. Conway and W. G. Pell, "Power limitations of supercapacitor operation associated with resistance and capacitance distribution in porous electrode devices," *J. Power Sources*, vol. 105, no. 2, pp. 81–169, 2002.

[14] L. Zubieta and R. Bonert, "Characterization of double-layer capacitors (DLCs) for power electronics applications," in *Proc. Conf. Rec. IEEE Ind. Appl. Conf., 33rd IAS Annu. Meeting*, vol. 2, Oct. 1998, pp. 1149–1154.

[15] R. Faranda, "A new parameters identification procedure for simplified double layer capacitor two-branch model," *Elect. Power Syst. Res.*, vol. 80, no. 4, pp. 363–371, 2010.

[16] V. Musolino, L. Piegari, and E. Tironi, "New full-frequency-range supercapacitor model with easy identification procedure," *IEEE Trans. Ind. Electron.*, vol. 60, no. 1, pp. 112–120, Jan. 2013.

[17] G. Navarro, J. Nájera, J. Torres, M. Blanco, M. Santos, and M. Lafoz, "Development and experimental validation of a supercapacitor frequency domain model for industrial energy applications considering dynamic behaviour at high frequencies," *Energies*, vol. 13, no. 5, p. 1156, Mar. 2020.

[18] H. Miniguano, A. Barrado, C. Fernández, P. Zumel, and A. Lázaro, "A general parameter identification procedure used for the comparative study of supercapacitors models," *Energies*, vol. 12, no. 9, p. 1776, May 2019.

[19] A. M. Nassef, A. Fathy, H. Rezk, and D. Yousri, "Optimal parameter identification of supercapacitor model using bald eagle search optimization algorithm," *J. Energy Storage*, vol. 50, Jun. 2022, Art. no. 104603.

[20] D. Raouti, S. Flazi, and D. Benyoucef, "Modeling and identification of electrical parameters of positive DC point-to-plane corona discharge in dry air using RLS method," *IEEE Trans. Plasma Sci.*, vol. 44, no. 7, pp. 1144–1149, Jul. 2016.

[21] Y. Zhao, W. Xie, Z. Fang, and S. Liu, "A parameters identification method of the equivalent circuit model of the supercapacitor cell module based on segmentation optimization," *IEEE Access*, vol. 8, pp. 92895–92906, 2020.

[22] Y. Wang, C. Liu, R. Pan, and Z. Chen, "Modeling and state-of-charge prediction of lithium-ion battery and ultracapacitor hybrids with a co-estimator," *Energy*, vol. 121, pp. 739–750, Feb. 2017.

[23] G. Sun, Y. Liu, R. Chai, F. Mei, and Y. Zhang, "Online model parameter identification for supercapacitor based on weighting bat algorithm," *AEU-Int. J. Electron. Commun.*, vol. 87, pp. 113–118, Apr. 2018.

[24] M. Ceraolo, G. Lutzemberger, and D. Poli, "State-Of-charge evaluation of supercapacitors," *J. Energy Storage*, vol. 11, pp. 211–218, Jun. 2017.

[25] L. Boulon, D. Hissel, A. Bouscayrol, M. C. Pera, and P. Delarue, "Multi physics modelling and representation of power and energy sources for hybrid electric vehicles," in *Proc. IEEE Vehicle Power Propuls. Conf.*, Sep. 2008, pp. 1–6.

[26] J. Van Mierlo, "Models of energy sources for EV and HEV: Fuel cells, batteries, ultracapacitors, flywheels and engine-generators," *J. Power Sources*, vol. 128, no. 1, pp. 76–89, Mar. 2004.

[27] E. Adib and H. Farzanehfard, "Soft switching bidirectional DC–DC converter for ultracapacitor–batteries interface," *Energy Convers. Manage.*, vol. 50, no. 12, pp. 2879–2884, Dec. 2009.

[28] N. Devillers, S. Jemei, M.-C. Péra, D. Bienaimé, and F. Gustin, "Review of characterization methods for supercapacitor modelling," *J. Power Sources*, vol. 246, pp. 596–608, Jan. 2014.

[29] K. Liu, C. Zhu, R. Lu, and C. C. Chan, "Improved study of temperature dependence equivalent circuit model for supercapacitors," *IEEE Trans. Plasma Sci.*, vol. 41, no. 5, pp. 1267–1271, May 2013.

[30] A. El Mejdoubi, H. Chaoui, H. Gualous, and J. Sabor, "Online parameter identification for supercapacitor state-of-health diagnosis for vehicular applications," *IEEE Trans. Power Electron.*, vol. 32, no. 12, pp. 9355–9363, Dec. 2017.

[31] A. Morandi, A. Lampasi, A. Cocchi, F. Gherdovich, U. Melaccio, P. L. Ribani, C. Rossi, and F. Soavi, "Characterization and model parameters of large commercial supercapacitor cells," *IEEE Access*, vol. 9, pp. 20376–20390, 2021.

[32] *2.7 V 3000 F Ultracapacitor Cell*. Accessed: May 22, 2022. [Online]. Available: https://maxwell.com/wp-content/uploads/2021/09/3003279.2_Final-DS_New-2.7V-3000F-Cell_20210406.pdf

SERGIO MARÍN-COCA received the bachelor's degree in aerospace engineering and the master's degree in space systems from the Universidad Politécnica de Madrid (UPM), Spain, in 2018 and 2020, respectively, where he is currently pursuing the Ph.D. degree in aerospace engineering, with his research focus being on the modeling of satellite's electrical power subsystems.

In 2020, he joined the Microgravity Institute "Ignacio Da Riva" (IDR/UPM), where he is a collaborator in space and civil aerodynamics projects. Since 2021, he has been an Assistant Professor with the School of Aeronautical and Space Engineering, UPM.

AMIR OSTADRAHIMI received the B.Sc. degree in electrical engineering from Shahid Beheshti University (aka the National University of Iran), Tehran, Iran, and the M.Sc. degree in power electronics engineering from the K. N. Toosi University of Technology, Tehran. He is currently pursuing the Ph.D. degree with the Department of Industrial Engineering, University of Rome "Tor Vergata," Italy.

His current research interests include modeling, controlling, and operating grid-connected converters and their application in modern energy grids. He is a frequent Reviewer of IEEE TRANSACTIONS ON ENERGY CONVERSION and IEEE TRANSACTIONS ON SUSTAINABLE ENERGY. He was selected as an "Outstanding Reviewer for IEEE TRANSACTIONS ON SUSTAINABLE ENERGY" in 2022.

STEFANO BIFARETTI (Member, IEEE) received the Ph.D. degree in electronic engineering from the University of Rome "Tor Vergata," Italy, in 2003.

In 2007, he has been a Research Fellow with the PEMC Group, University of Nottingham, U.K. Since 2015, he has been an Associate Professor of power electronics and electrical drives with the Department of Industrial Engineering, University of Rome "Tor Vergata." He has published more than 100 papers in international journals and conference proceedings. His recent research interests include the design, modeling, and control of power electronics multi-port multi-level converters, solid-state transformers, fast charging stations, and high-power supplies for nuclear fusion energy generators. He is serving as the Transactions Papers Review Chair for the IAS Industrial Power Converters Committee for the IEEE TRANSACTIONS ON INDUSTRY APPLICATIONS.

ELENA ROIBÁS-MILLÁN received the M.Sc. and Ph.D. degrees in aerospace engineering from the Universidad Politécnica de Madrid (UPM), Spain, in 2011 and 2014, respectively.

She started at UPM, as a Researcher through an NPI grant awarded by the European Space Agency, where she developed her Ph.D. dissertation. She has performed several research stays in ESA/ESTEC (TEC-MSS Section) and the Space Systems Section of Airbus DS, Spain. Since 2015, she has been a Professor with UPM. Since 2015, she has been with the Microgravity Institute 'Ignacio Da Riva' (IDR/UPM) and the research group 'Space Systems Development and Testing.' Additionally, she is the Deputy Director of the Aerospace Systems, Air Transport and Airports, ETSIAE (UPM). She has participated in several space projects (SEOSAT/INGENIO, ExoMARS, and Solar Orbiter) and the Technical Director of the UPMSat Program of IDR.

SANTIAGO PINDADO received the M.Sc. and Ph.D. degrees in aerospace engineering from the Technical University of Madrid (UPM—Universidad Politécnica de Madrid), Spain, and the Ph.D. degree in experimental and civil aerodynamics from the Instituto Universitario de Microgravedad "Ignacio Da Riva" (IDR/UPM), in 1999.

He worked with SENER Engineering Company, from 1996 to 1999, being involved in aerodynamics and fluid mechanics simulations. He has been a Professor with UPM, since 2003. In 2008, he became responsible for the UPMSat-2 power subsystem. Additionally, he has held different executive positions at UPM, as the Deputy Director of the IDR/UPM Institute, the Head of the Studies of the UPM Master Program in Space Systems, and the Technical Director of the LAC-IDR/UPM Calibration Laboratory.

Open Access funding provided by 'Università degli Studi di Roma ''Tor Vergata''' within the CRUI CARE Agreement